Interaction of Aerosol Particles and Clouds

Andrea Flossmann

Interaction of Aerosol Particles and Clouds

ANDREA I. FLOSSMANN

Laboratoire de Météorologie Physique, Université Blaise Pascal - CNRS - OPGC, Aubiere, France

(Manuscript received 29 October 1996, in final form 4 August 1997)

ABSTRACT

With the spectral scavenging and microphysics model DESCAM coupled to a 2D dynamic framework the transport and scavenging of aerosol particles by a medium-sized convective cloud are investigated. For typical marine conditions the author has found a depletion of the marine boundary layer of about 70%. Also, about 70% of the vented up aerosol particle mass entered cloud drops due to nucleation. For these simulations the author found an increase in relative humidity, as well as number concentration of Aitken and large and giant particles near cloud top. The increase in relative humidity and large and giant particle concentration was coupled to cloud outflow regions, while the increase in Aitken particles can be attributed to lifting of free tropospheric air due to cloud-top rising. Sensitivity tests varying the number of free tropospheric sulfate particles changed the number of cloud drops but had little effect on precipitation formation and evolution.

1. Introduction

Aerosol particles and clouds interact in a variety of different ways. It is commonly understood now that aerosol particles provide the nuclei for cloud droplet formation. Consequently, aerosol particles directly determine the number of drops formed. This, in turn, affects the evolution of the cloud, precipitation formation, and the radiative cloud properties. This ''indirect'' radiative effect has been recognized to be climatically relevant (e.g., Twomey 1977) and, thus, the relation of clouds and aerosol particles has received renewed attention. This interaction is discussed, especially over the ocean, with respect to an enhanced DMS (dimethyl sulfite) production, which might increase the number of small particles, increase the number of cloud drops, and then increase the albedo of clouds (Charlson et al. 1987). The issue here is not only whether an enhanced DMS production would change the radiative properties of clouds, but also where and how this new particle production might proceed. Here, clouds are anticipated to play an essential role. Hegg et al. (1990, 1991), Radke and Hobbs (1991), and Perry and Hobbs (1994), among others, have observed an enhanced concentration of Aitken particles in the vicinity of the top of stratocumulus as well as small cumulus clouds and have suggested a mechanism of homogeneous–bimolecular nucleation of new particles. The homogeneous–bimolecular nucleation is the formation of new droplets or particles produced by interaction between two vapor species without the aid of a foreign nucleus or surface. The nucleation of sulfuric acid droplets from the H_2O–H_2SO_4 vapor system has been proposed as an important source of small aerosol particles (e.g., Junge 1963; Kiang et al. 1973; Middleton and Kiang 1978). Conditions favorable for this mechanism are low surface area of existing aerosol particles, cold temperatures, SO_2 concentrations larger than 25 pptv, and high relative humidities ($>$70%), which might be found in the vicinity of marine clouds (Hegg et al. 1990). Other authors (e.g., Baumgardner et al. 1996) have found an increase of particles larger than 0.3-μm diameter in the vicinity of marine clouds. For all these measurements the question arises whether the increase of the observed particles could be due to simple cloud transport (venting) and transformation or whether environmental conditions were conducive to new particle formation or perhaps some combination of air motion and new particle formation.

The effect of cloud venting of *gases* has been shown to be important by numerous authors for different clouds and cloud systems. A comprehensive review of observational and modeling studies on cloud venting by a wide variety of cloud types ranging from ordinary cumuli to ordinary cumulonimbi, mesoscale convective systems, and tropical and extratropical cyclones has been given by Cotton et al. (1995). Aerosol particles, however, are not just vented up but interact with the cloud in a variety of different ways.

In order to study the aerosol particle–cloud interaction we have applied our DESCAM, that is, the detailed scavenging and microphysical model (e.g., Flossmann et al. 1985; Flossmann and Pruppacher 1988; Flossmann 1994) embedded in the two-dimensional dynamics pro-

Corresponding author address: Dr. Andrea I. Flossmann, Laboratoire de Météorologie Physique, Université Blaise Pascal - CNRS - OPGC, 24 avenue des Landais, Aubiere, F-63177 Cedex, France.
E-mail: flossman@opgc.univ-bpclermont.fr

vided by the model of Clark and coworkers (e.g., Clark 1977, 1979; Clark and Gall 1982; Clark and Farley 1984; Hall 1980) to a moderate warm convective cloud developing on GATE day 261. The GATE (GARP Atlantic Tropical Experiment) campaign was performed in 1974 off the coast of Africa in the ITCZ. The measurements showed that the well-mixed boundary layer had a depth of about 500 m (Warner et al. 1979; Nicholls and LeMone 1980). Above, there was a moist layer reaching about 2.2 km, capped by a stable layer where the air was very dry. Brümmer (1978) showed that this inversion layer was typical of an environment in this geographical region disturbed by previous convection and that these inversions normally did not persist for more than a couple of hours. Consequently, these inversions would not inhibit the exchange of air masses between the moist layer and the higher troposphere.

We have used this dynamical situation already to study the transport of gases of different solubilities from the well-mixed boundary layer to the free troposphere by this moderate-sized convective cloud (Flossmann and Wobrock 1996).

In the present study we will focus on the transport and scavenging of aerosol particles due to cloud processes. All interactions with gas uptake as well as new particle formation was purposely disregarded.

For the reference case we used a typical marine situation. In the marine boundary layer (MBL) the aerosol size distribution represents a mixture of numerous small sulfate particles and few large ones consisting of sea salt (Fitzgerald 1991). This aerosol particle spectrum was set to exist homogeneously mixed in the entire MBL. Above the MBL, we assumed that the distribution of sulfate decreased exponentially while the sea salt was set to zero. This was assumed to create a ''textbook situation'' as sea salt is produced at the sea surface while sulfate particle nucleation is possible to occur everywhere in the atmosphere (Fitzgerald 1991).

In order to be able to separate transports across the MBL from transports in the free troposphere and also to be able to study the influence of increased or reduced sulfate particle nucleation in the free troposphere, we have performed two additional sensitivity tests. In the first we have purposely set all initial aerosol material above the MBL to zero. In a second test we have doubled the number of sulfate aerosol particles aloft. Below, the model and the initial conditions will be presented and the results will be discussed.

2. Model description

As discussed in detail by Flossmann and Pruppacher (1988), the basic framework employed in the present study is a two-dimensional slab-symmetric version of the three-dimensional model developed by Clark and coworkers (e.g., Clark 1977, 1979; Clark and Gall 1982; Clark and Farley 1984; Hall 1980). The DESCAM model is discussed in Flossmann et al. (1985, 1987). There, the aerosol particles are represented by their size spectra. Apart from dynamical processes, changes to the number of particles of a certain size occur as a result of droplet activation, humidity changes, and impaction scavenging by drops. The nucleated drops then grow by condensation or evaporate, collide and coalesce, and eventually break up. During their lifetime they further scavenge particles and the scavenged pollutant mass is redistributed through the microphysical processes. The extension of this microphysical and scavenging model to the scavenging of two different types of aerosol particles [e.g., $(NH_4)_2SO_4$ and NaCl for marine air masses] is described in Flossmann (1991) and the inclusion of effects of gaseous H_2O_2 and O_3 on the uptake and oxidation of SO_2 was presented in Flossmann (1994). Currently, the model contains prognostic equations for 11 distribution functions as summarized in Table 1. For further details on the terms changing the density distribution functions see Flossmann et al. (1985) and Flossmann (1994).

For the model results presented here, however, the gas phase concentrations were set to zero and only the interaction of drops and aerosol particles was studied. The model covered a domain of 10 km in the vertical and 20 km in the horizontal. The grid spacings were

TABLE 1. Eleven density distribution functions as used in the DESCAM model with m being drop mass and m_{AP} being the aerosol particle mass; the drop and aerosol particle categories are logarithmically equally spaced with a mass doubling every second category.

Density distribution function		Number of classes, min–max radius (μm)
f_d (m)	Drop number density distribution function	57, 4–2580
$g_{APd,(NH4)2SO4}$ (m)	Mass density distribution function for $(NH_4)_2SO_4$ particles in the drops	57, 4–2580
$g_{APd,NaCl}$ (m)	Mass density distribution function for NaCl particles in the drops	57, 4–2580
$g_{Gd,S(4)}$ (m)	Mass density distribution function for the sulfur species S(4) in the drops	57, 4–2580
$g_{Gd,S(6)}$ (m)	Mass density distribution function for the sulfur species S(6) in the drops	57, 4–2580
$g_{Gd,H2O2}$ (m)	Mass density distribution function for H_2O_2 gas in the drops	57, 4–2580
$g_{Gd,O3}$ (m)	Mass density distribution function for O_3 gas in the drops	57, 4–2580
$f_{APa,(NH4)2SO4}$ (m_{AP})	Aerosol particle number density distribution function for $(NH_4)_2SO_4$ particles in the air	81, 10^{-3}–10
$f_{APa,NaCl}$ (m_{AP})	Aerosol particle number density distribution function for NaCl particles in the air	81, 10^{-3}–10
$g_{APa,(NH4)2SO4}$ (m_{AP})	The mass density distribution function for $(NH_4)_2SO_4$ particles in the air	81, 10^{-3}–10
$g_{APa,NaCl}$ (m_{AP})	The mass density distribution function for NaCl particles in the air	81, 10^{-3}–10

TABLE 2. Parameters for the maritime aerosol particle distribution as given in Eq. (1); n_i: total number of aerosol particles per cubic centimeter; R_i: geometric mean aerosol particle radius in μm; σ_i: standard deviation in mode i: chemical composition and scale height H_i (in m) of the aerosol particle modes; the number concentrations above 400-m altitude for the three cases considered.

Mode i	n_i	R_i	$\log\sigma_i$	Chemical compound	H_i (>400 m)	Case 1 (>400 m)	Case 2 (>400 m)	Case 3 (>400 m)
1	133	0.0039	0.657	$(NH_4)_2SO_4$	3000	$1 \cdot n_i$	$0 \cdot n_i$	$2 \cdot n_i$
2	66.6	0.1330	0.210	$(NH_4)_2SO_4$	3000	$1 \cdot n_i$	$0 \cdot n_i$	$2 \cdot n_i$
3	3.06	0.2900	0.396	NaCl	—	$0 \cdot n_i$	$0 \cdot n_i$	$0 \cdot n_i$

$\Delta z = 200$ m and $\Delta x = 400$ m resulting in 52×52 grid points. The overall time step was $\Delta t = 5$ s with a possible reduction in the condensation routine. The time step represents a compromise between rapid processes like cloud microphysics and turbulence and the computational effort to integrate such a large model over a 1-h time period.

3. Initial conditions

The initialization of the present model is the same as that in Flossmann (1991, 1994) and Flossmann and Wobrock (1996) with the exception of the initial concentrations for the aerosol particles: The sounding was taken at day 261 (18 September 1974) of the GATE campaign at 1200 UTC. Our 2D model domain was oriented north–south, as this was the main wind direction. In the lowest 2 km and above 6 km the wind was southerly, while in between the wind was northerly.

The initial aerosol particle spectrum was assumed to be of maritime type consisting of a superposition of three lognormal distributions as proposed by Jaenicke (1988):

$$\frac{dN}{d\ \ln r} = f_{\mathrm{AP}a}(\ln r) = \sum_{i=1}^{3} \frac{n_i}{(2\pi)^{1/2}\log\sigma_i \ln 10}\exp\left(-\frac{[\log(r/R_i)]^2}{2(\log\sigma_i)^2}\right). \quad (1)$$

The two small modes $i = 1$ and 2 were assumed to consist of $(NH_4)_2SO_4$ particles and the large mode $i = 3$ was set to hold only NaCl particles. The parameters are summarized in Table 2. This aerosol particle size distribution was assumed to exist homogeneously throughout the MBL, that is, in the lower 400 m for the case considered. For the height dependency above the MBL three different scenarios were studied. In the first case, the $(NH_4)_2SO_4$ particles were assumed to decrease exponentially with height with a scale height of 3 km, while the NaCl particles were assumed to be zero above the boundary layer. In the second case all aerosol particle concentrations above 400 m were assumed to zero, and in the third case the $(NH_4)_2SO_4$ particles above 400 m were doubled with respect to case 1 while the NaCl concentration was still assumed to zero.

The cloud was driven by a surface sensible and latent heat flux as a percentage of the incoming solar radiation. The method is described in Flossmann (1991).

4. Model results

A similar aerosol particle concentration and distribution as the one used here coupled with the same dynamical situation was studied already in Flossmann (1991, 1993). Then, we compared the results with the meteorological observations made during the GATE campaign and typical observations of aerosol particle scavenging in marine tropical oceans and found a reasonable agreement. Consequently, this aspect will not be studied here again. Instead, we will focus on the aerosol–cloud interaction concerning mass as well as number of aerosol particles.

The model simulation started at 1200 UTC. After 26 min of model time a cloud had formed. After 14 min of cloud life time the first rain fell from cloud base and after 19 min of cloud life time the first rain reached the ground.

Figure 1 shows the drop number concentration in the cloud for the three cases considered. The different number of isoplethes in the three figures immediately suggests that case 3 (Fig. 1c) forms the highest droplet concentrations and case 2 (Fig. 1b) the lowest. The droplet concentration is determined by CCN entering cloud base and from entrainment of particles at cloud boundaries.

Figure 2 gives the net mass transport and scavenging associated with the cloud. [For a description of the calculation of the fluxes see Flossmann and Wobrock (1996); the fluxes do not add to zero as changes of the reservoirs go along.] We see here that in all three cases the net mass inflow and outflow through the other cloud boundaries is small compared to what enters via the cloud base. Investigating the correlation of the venting of aerosol particle number and mass through the MBL with the droplet formation we note two things.

The first is that the total mass of aerosol particles activated and nucleating to drops in cloud (nucleation scavenging) is almost always larger than the net venting. This is due to the fact that the net venting is composed of an upgoing mass transport and a downgoing mass transport. The downgoing transport takes place in the cloud-free air at the sides and is associated with the downdrafts (compare Figs. 3c and 4c of Flossmann and Wobrock 1996). The upgoing and downgoing components of aerosol particle transport are explicitly given in Table 3 and the subtraction of the two numbers gives the net venting of Fig. 2. We have to explain here that in contrast to Flossmann and Wobrock (1996), where we studied the venting of gases directly across cloud

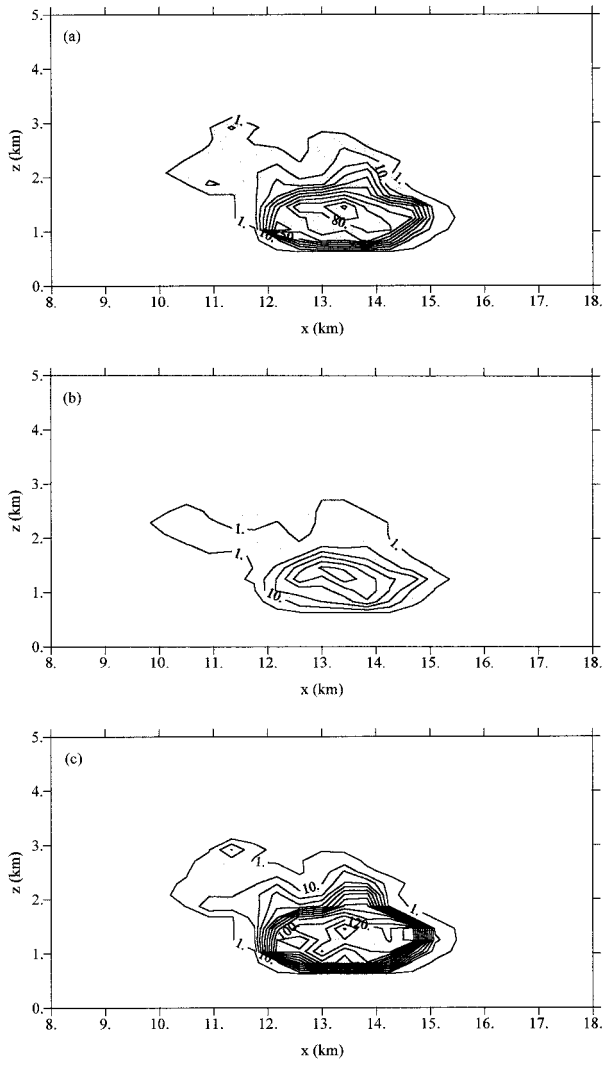

FIG. 1. Drop number concentration in per cubic centimeter after 45 min of model time (19 min of cloud lifetime) for the three cases considered; contour spacing 10 cm^{-3}, the outmost contour line is 1 cm^{-3}, the shaded area is the visible cloud ($q_c > 0.1$ g kg^{-1}).

base, here we are studying the transport across the interface MBL–free troposphere at 400 m. This is caused by the fact that numerous aerosol particles become activated at cloud base and, thus, the flux calculations directly across cloud base gave erroneous results. For the gas case (Flossmann and Wobrock 1996), however, the upward venting across cloud base agreed with a transport across 400 m to within 7%. In Table 4, we have computed values for four scavenging efficiencies pertaining to the end time of our computation as

E_1 = cumulative nucleation scavenging/cumulative aerosol mass scavenged by nucleation and impaction;
E_2 = cumulative aerosol particle mass in surface rain/cumulative aerosol mass scavenged by nucleation and impaction;

TABLE 3. Total up- and downgoing mass and number of aerosol particles at the height of the marine boundary layer (MBL = 400 m) integrated over the simulation period of 1 h; the values pertain to a 2D cloud of 1-m depth.

Case	Integrated upgoing mass of AP (g m^{-1})	Integrated downgoing mass of AP (g m^{-1})	Integrated upgoing number of AP (m^{-1})	Integrated downgoing number of AP (m^{-1})
1	227	66	$3.1\ 10^{13}$	$1.9\ 10^{13}$
2	232	30	$2.0\ 10^{13}$	$2.5\ 10^{12}$
3	341	149	$5.9\ 10^{13}$	$4.7\ 10^{13}$

E_3 = cumulative impaction scavenging/cumulative aerosol particle mass in surface rain; and
E_4 = cumulative nucleation scavenging/total aerosol particle mass transport upward across the marine boundary layer.

We see that the values for E_1–E_3 give the same orders of magnitude as obtained before for the simulation of the GATE cloud and a cloud in the Hawaiian rainband as presented in Flossmann (1991). The difference in the numbers essentially reflect the differences in nucleation scavenging. Calculating the ratio of nucleation scavenging to total upward venting of aerosol particle mass E_4, we find for the three cases 73%, 52%, and 61%.

The second thing we note, looking at Table 3, is that the upgoing mass flux is of the same order as the initial aerosol particle mass loading of the MBL (240 g m^{-1}, Fig. 2) for cases 1 and 2, but in the third case the initial aerosol particle mass loading is greatly exceeded by the upward mass flux. If we consider, however, only the net venting number (upgoing mass − downgoing mass, given in Fig. 2), we obtain a ratio of transport/initial loading of 67%, 84%, and 80%, respectively, which gives the same order of magnitude we already found for the depletion of gas from the MBL by this convective cloud (~60%; Flossmann and Wobrock 1996). Thus, we can conclude that the compensating downdraft at the cloud edges plays an important role in replenishing the MBL and, thus, increasing the integrated masses transported upward and downward. The least efficient replenishment can be found in case 2 (Table 3) as initially no particles existed in the free troposphere. Consequently, the net depletion of the MBL is largest resulting in the largest ratio of transport/initial loading (84%).

The role of the compensation downdraft also explains the difference in droplet number concentrations in the cloud. The initial MBL concentration was identical, sug-

TABLE 4. Scavenging efficiencies for the three cases considered as defined in the text.

	Case 1	Case 2	Case 3
E_1	89.2	88.2	89.8
E_2	39.3	46.6	36.7
E_3	27.3	25.2	27.7
E_4	73.0	51.6	60.9

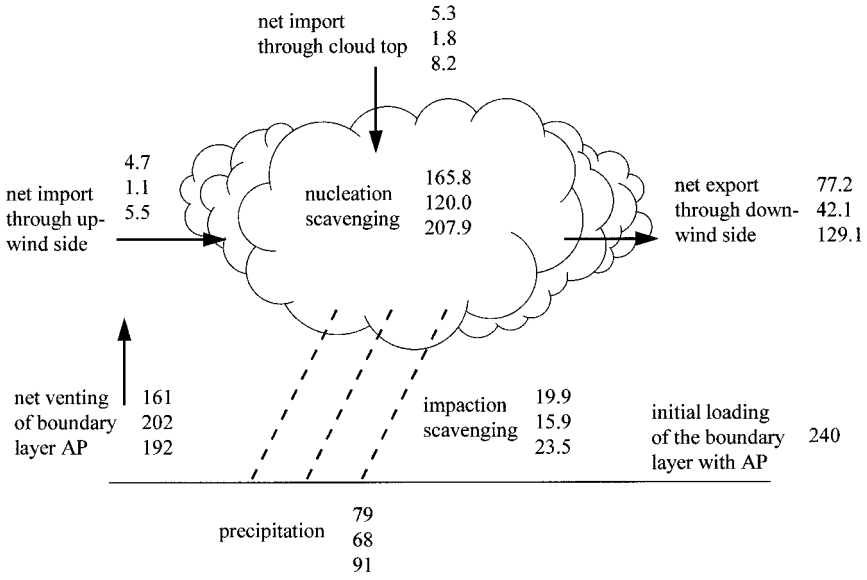

FIG. 2. Net mass transport and scavenging integrated over the 1 h of simulation time; the upper number pertains to case 1, the second to case 2, and the third to case 3, the values are given in g m^{-1} pertaining to a 2D cloud of 1-m depth; for the transport the arrows give the net direction.

gesting an identical early cloud droplet number concentration. But as soon as the ascending movement starts, that is, even prior to cloud formation, the compensating downdraft develops mixing air containing aerosol particles from above the boundary layer into the MBL. This downward mixing can be seen in Table 3 where the downward particle number transport is largest for case 3 and more than one order of magnitude smaller for case 2. For case 2 initially no aerosol particles existed above the boundary layer. Consequently, all particles mixed back must previously have been vented upward from the MBL. The subsiding air partially reenters the updraft core and is responsible for the fact that even immediately after formation the cloud drop number concentrations for the three cases considered differ. Adding to this difference is that initially the cloud base is around 800-m altitude and only later (after 50 min) subsides to 400 m due to evaporating precipitation. Consequently, boundary layer air is mixed between 400- and 800-m altitude with above boundary layer air before entering cloud base.

Even though the droplet concentration in the three cases are different, the overall dynamics of the clouds differs only very little. The most significant changes are reflected in the evolution of precipitation. But even there the development is rather similar, as can be seen from Fig. 3a. Figure 3 shows the rain rate and wet deposition of the two chemical aerosol species. We see that the evolution of the rainfall and total precipitation (1.71 mm, 1.87 mm, and 1.66 mm) is quite similar. The same applies for the wet deposition rate of NaCl (Fig. 3c), which only stems from the MBL. The differences in the wet deposition of $(NH_4)_2SO_4$ reflects, however, the different initial vertical distribution of aerosol particles above the MBL, yielding the smallest values for case 2 and the largest for case 3. The reason for the similar evolution of the rainfall rate can be attributed to the fact that for all three cases the initial aerosol particle distribution stays in the range of typical marine concentrations, which were defined by the identical initial loading of the MBL. Marine aerosol particle spectra are known to produce precipitation rather easily due to generally low droplet concentration and rapid collision and coalescence (e.g., Hobbs 1993). Only if this marine aerosol distribution is significantly perturbed, for example, by anthropogenic influence, a change of the rain formation potential can be anticipated. This has been found, for example, for the case of ship tracks (Hobbs 1993).

After having studied the effect of the different aerosol particle distributions on cloud formation and evolution we will now investigate the effect of the cloud on the distribution of the aerosol particles in the air. Due to the different anticipated behavior of Aitken particles and large and giant particles, we will look at these two species separately. Figure 4 displays the change in the relative humidity field and in the field of small ($r < 0.1$ μm) and large ($r > 0.1$ μm) particles with respect to the initial fields. For the relative humidity (Fig. 4a) we see, in general, an increase in the upper part of the atmosphere and a decrease in the lower part, except for the region of the cloud itself where the relative humidity always is above 100%. This redistribution is due to the fact that the cloud pumps water vapor from the boundary layer into the cloud. Next to cloud top where the vertical motion drops to zero we have an outflow at the edges of the cloud, which is responsible for a moistening of the adjacent cloud free air. With the associated downdrafts at the sides the water vapor is transported downward toward the sea surface. This, however, does not show in an increase in relative humidity since

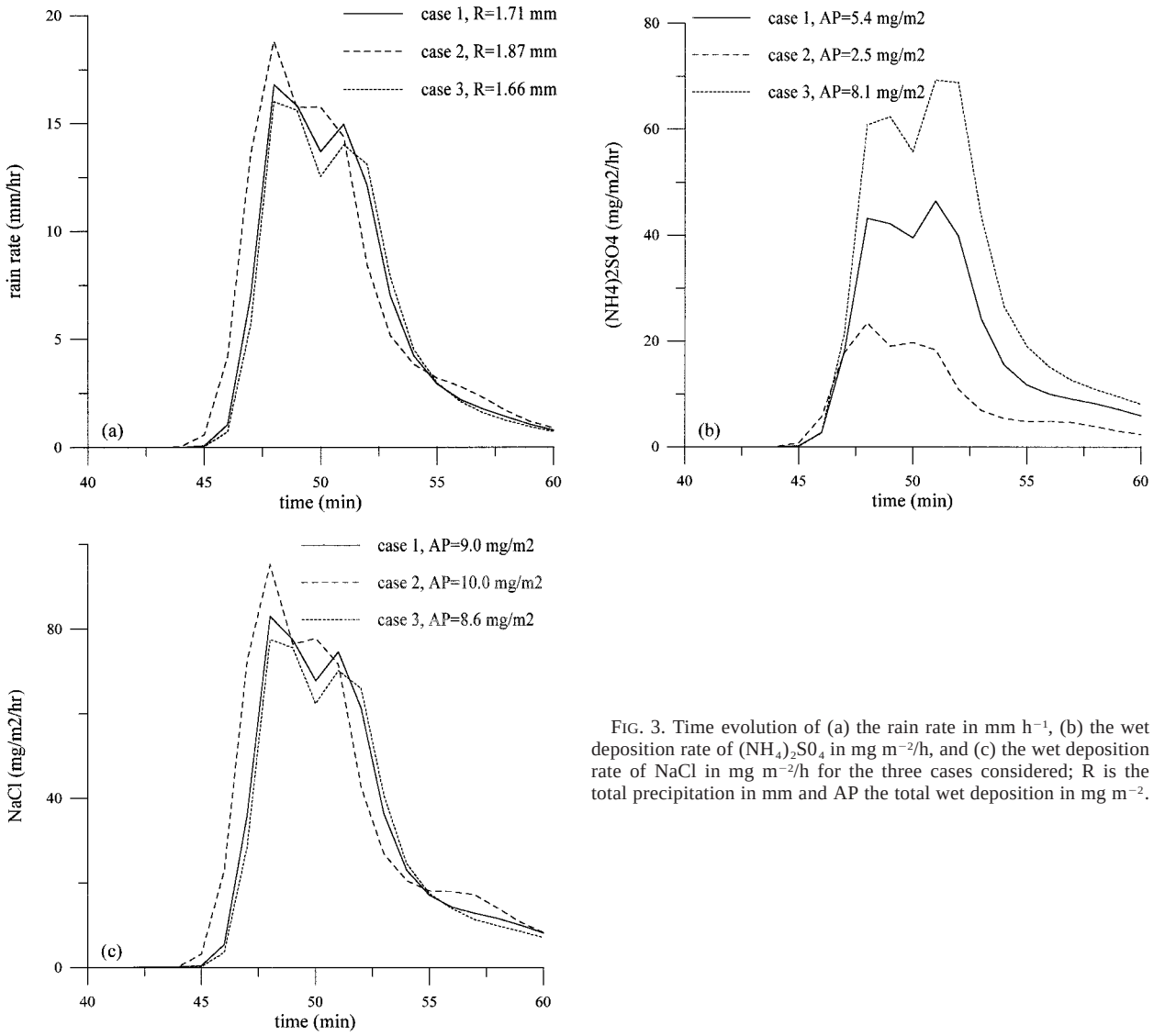

FIG. 3. Time evolution of (a) the rain rate in mm h^{-1}, (b) the wet deposition rate of $(NH_4)_2S0_4$ in mg m^{-2}/h, and (c) the wet deposition rate of NaCl in mg m^{-2}/h for the three cases considered; R is the total precipitation in mm and AP the total wet deposition in mg m^{-2}.

the downdraft is also associated with a general warming of the air. Next to the cloud top we find now relative humidities of 70%–80%.

Figures 4b and 4c give the change in the aerosol particle concentrations. Both the small and the large particle concentrations experience an increase above cloud top. The reasons, however, are different and will be discussed below separately for Figs. 4b and 4c.

Figure 4b shows the change in the Aitken particle concentration. Due to the relatively high supersaturation ($S_{max} \sim 2\%$) created by the cloud, some of the Aitken particles serve as cloud condensation nuclei. Consequently, we see a decrease in the region of the cloud and its immediate vicinity. Besides this, we detect an increase of Aitken particle concentration above 3 km. This is above the region affected by the humidity increase (compare Fig. 4a) and is situated inside the inversion. These particles obviously belong to the air above the boundary layer and were probably lifted aloft with the rising cloud top. This is emphasized by Fig. 5a, which shows the total number of Aitken particles for case 2. As initially the air above the MBL was particle free, the number concentrations given here already represent the changes. We see here that no layer of Aitken particles exists above 3 km. Instead, we see an increase of the number of Aitken particles in the region of the cloud itself. This is caused by the venting of the cloud and that only a small part of the Aitken particles served as CCN. The increase of the particle concentration in cloud due to venting is overcompensated in cases 1 and 3 (see Fig. 6a) by the nucleation scavenging going on at the same time, that imposed a net decrease compared to the original values.

Figure 4c shows the change in the large and giant

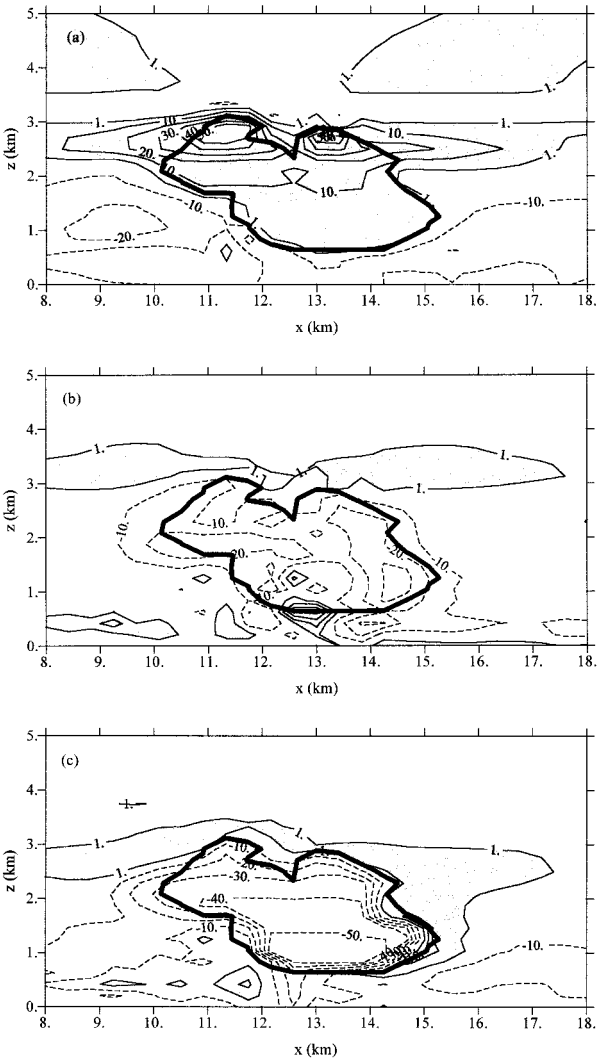

FIG. 4. Difference for case 1 in (a) the relative humidity in percent, (b) the number concentration of small aerosol particles (radius < 0.1 μm) in per cubic centimeter, and (c) the number concentration of large aerosol particles (radius > 0.1 μm) in per cubic centimeter after 45 min of model time (19 min of cloud lifetime) compared to the initial state at $t = 0$ min; for (a) the contour spacings are 10%, the solid line represents a higher relative humidity and the dashed line represents a lower relative humidity; the shaded area gives the region of increases larger 1%; for (b) and (c) the contour spacings are 10 cm^{-3}, the solid line represents an increase and the dashed line represents a decrease in number concentration; the shaded area gives the region of increases larger than 1 cm^{-3}, the thick line is the contour of the visible cloud ($q_c > 0.1$ g kg^{-1}).

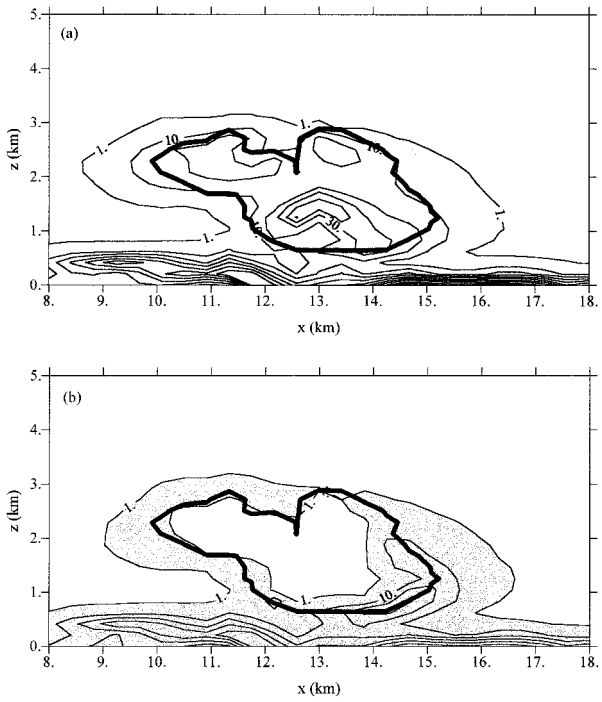

FIG. 5. For case 2 (a) the number concentration of small aerosol particles (radius < 0.1 μm) in per cubic centimeter, and (b) the number concentration of large aerosol particles (radius > 0.1 μm) in per cubic centimeter after 45 min of model time (19 min of cloud lifetime); the contour spacings are 10 cm^{-3}, the shaded area gives the region larger 1 cm^{-3}; the thick line is the contour of the visible cloud ($q_c > 0.1$ g kg^{-1}).

particle concentration. These particles mainly consist of NaCl and only a small fraction of $(NH_4)_2SO_4$ and their number concentration is much smaller than that of the Aitken particles. These particles all served as cloud condensation nuclei and, thus, their number concentration in the cloud is reduced to zero (cf. Fig. 5b for case 2). Looking at Fig. 4c we see an increase of the large particle concentration above the cloud and at its ''right edge.'' This right edge is associated with the outflow edge of the 2D cloud due to the imposed horizontal wind shear (cf. Figs. 3d and 4d of Flossmann and Wobrock 1996). At this edge and near cloud top, cloud drops leave the cloud and are evaporated completely, releasing an aerosol particle nucleus back into the cloud-free atmosphere. This aerosol particle obviously belongs to the larger particle kind since these were the particles that formed the drops and even increased in size due to in-cloud processes like collision and coalescence of drops (Flossmann et al. 1987). Comparing with Fig. 4a we see that these regions of enhanced particle concentrations are roughly associated with the regions of enhanced relative humidity as both result from cloud outflows. Roughly the same behavior, only more pronounced due to higher input concentration, can be found for case 3. The effect for case 2, however, is smaller. This is due to two reasons: The first is that the number of activated particles was less to begin with and thus would also produce less evaporated nuclei (see Fig. 1b). Second, we have to consider that a large number of the particles creating the increase in cases 1 and 3 actually are not evaporated drops but initial Aitken particles that have grown due to the increase in relative humidity by detrained water vapor to particles larger that 0.1 μm. These particles will be less numerous in case 2, which was initialized with no particles in the cloud region.

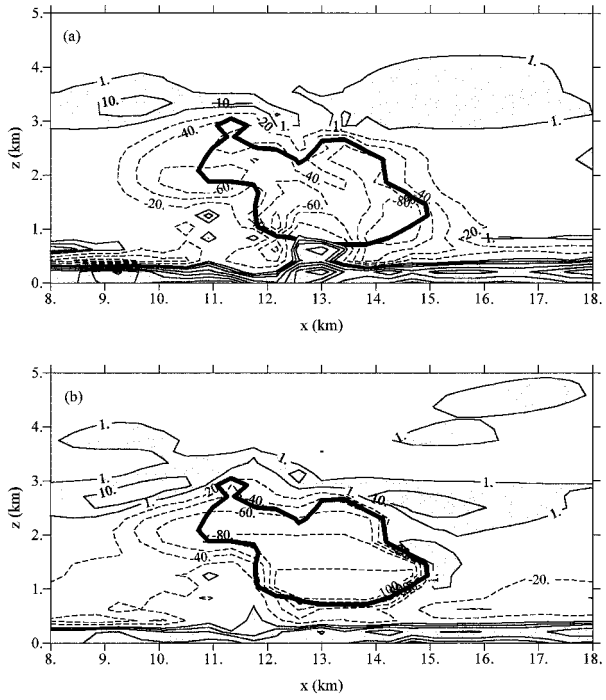

FIG. 6. Difference for case 3 in (a) the number concentration of small aerosol particles (radius < 0.1 μm) in per cubic centimeter, and (b) the number concentration of large aerosol particles (radius > 0.1 μm) in per cubic centimeter after 45 min of model time (19 min of cloud lifetime) compared to the initial state at $t = 0$ min; the positive contour spacings (solid line) are 10 cm^{-3}, the negative contour spacings (dashed line) are 20 cm^{-3}, and the shaded area gives the region of increases larger 1 cm^{-3}; the thick line is the contour of the visible cloud ($q_c > 0.1$ g kg^{-1}).

Furthermore, we note in Fig. 6 for case 3 an increase of both small and large particles in the MBL. This increase is a result of the initialization imposing a discontinuity in the particle concentration at 400 m as a doubling of the concentration aloft is introduced. Even though the concentration decreases exponentially aloft, the discontinuity is sufficient to create locally a strong gradient reponsible for the increase of particle concentration in the MBL.

5. Summary and conclusions

We have used our DESCAM model coupled to a 2D dynamic framework to study the transport and scavenging of aerosol particles in the marine atmosphere by a medium-sized convective cloud. We have studied three cases with an identical initial aerosol particle boundary layer concentration. Above the MBL the sea salt concentration was always assumed to zero, while the sulfate concentration varied. We found for the cases studied that the precipition formation and evolution varied only slightly even though the number of cloud drops produced differed. We can conclude that in a clean marine atmosphere a reduced or enhanced sulfate production in the free troposphere will not significantly change the precipitation properties within the range of values considered. However, changes in the cloud radiative properties can be anticipated as these depend heavily on drop concentration as well as size.

We further found an important upward and downward transport of aerosol particles across the MBL caused by the cloud. The net result of this transport depleted about 70% of the aerosol from the MBL, which is slightly higher than the 60% previously found for gases (Flossmann and Wobrock 1996). In addition, a downward transport of particles was found in all cases replenishing the MBL and, thus, preventing a complete depletion of the model MBL. We studied the mass transport and scavenging of particles by the cloud and found that roughly 70% of the particle mass vented upward from the MBL entered the cloud drops due to nucleation. Concerning these numbers a certain caution, however, is advised as they were obtained by a 2D model dynamics in a limited model domain. Thus, we can expect a certain dependancy on the model architecture, the domain size, and also the case studied. However, we are convinced that the general features will reappear, as further sensitivity studies already indicate.

This is also true for the results concerning the aerosol particle concentration fields around the cloud. Here, we find evidence for an enhancement in both Aitken particles and large and giant particles. Our simulation confirms the measurements, for example, of Baumgardner et al. (1996), who have found an increase of particles larger than 0.3-μm diameter at the outflow edges of a cloud. Here particles larger than 0.1-μm radius also increased in number concentration. This region was also associated with an increase in water vapor concentration and/or relative humidity. These particles were residues of evaporated drops or former Aitken particles that had assimilated significant water vapor due to the moistening of the air by detrainment.

For the Aitken particles we also noted an increase that is, however, decoupled from the region of enhanced relative humidity or large particle concentration. This enhancement resulted from unactivated free tropospheric aerosols lifted aloft by the rising cloud top. It is interesting to note here that this enhanced layer of Aitken particles is significantly higher than cloud top as was observed also, for example, by Hegg et al. (1990). They associated this increase in particle concentration to new particle formation on site due to homogeneous–bimolecular nucleation. We certainly cannot rule out this phenomenon especially as they measured increases of several hundred particles per cubic centimeter while our increases only range between 1 and 10 particles per cubic centimeter. Our model, however, considers only transport and cloud microphysical processes. Still we have found an increase of both Aitken and large particles in the regions where they have been observed. We can imagine a scenario with an initial pollution layer or a region of new particle production prior to cloud formation in the region between the height of the MBL

and the transient inversion. Then the transport processes associated with the cloud might cause an accumulation of these particles near cloud top and produce there significantly higher concentrations matching more closely the observed values. Certainly, we have to reconsider the statement of Perry and Hobbs (1994) that cloud outflow air is rich in relative humidity and gases but poor in particles due to incloud nucleation scavenging. Our calculations have shown that in the outflow region cloud droplets evaporate, releasing an aerosol particle residue. Thus, this air still offers a certain aerosol particle surface. In addition, our calculations concerning the venting of SO_2 by this cloud (Flossmann and Wobrock 1996) have shown that the SO_2 concentrations next to cloud top have been reduced due to uptake inside the cloud drops. These effects might be less favorable for new particle formation directly adjacent to cloud top.

In addition, we have to consider that new particle formation is supposed to occur on the timescale of hours to days (Hoppel 1992; Perry and Hobbs 1994). Consequently, new particle formation adjacent to the top of a cumulus cloud like the one considered with lifetimes on the order of 1 h is unlikely to yield the increase of a factor of 2 in the Aitken particle concentration as observed, for example, by Radke and Hobbs (1991) for small cumulus clouds.

Acknowledgments. The author acknowledges with gratitude the support by the European Community under EV5V-CT93-0313 / ENV4-CT95-0012 / ENV4-CT95-0117. She is solely responsible for the content of this manuscript. The author wants to thank Bob Charlson for useful discussions and the suggestions for parts of this paper. The calculations for this paper have been done on the CRAY C98 and C94 of the Institut du Développement et des Ressources en Informatique Scientifique (IDRIS, CNRS) in Orsay (France) under project 940180. The author acknowledges with gratitude the hours of computer time and the support provided. Furthermore, the author acknowledges the support provided by the French national program PATOM.

REFERENCES

Baumgardner, D., W. A. Cooper, and L. F. Radke, 1996: The interaction of aerosol with developing maritime and continental cumulus clouds. *Proc. of the 12th ICCP,* Zurich, Switzerland, ICCP, 308–311.

Brümmer, B., 1978: Mass and energy budgets of a 1 km high atmospheric box over the GATE C-scale triangle during undisturbed and disturbed weather conditions. *J. Atmos. Sci.,* **35,** 997–1011.

Charlson, R. J., J. E. Lovelock, M. O. Andreae, and S. G. Warren, 1987: Oceanic phytoplankton, atmospheric sulphur, cloud albedo and climate. *Nature,* **326,** 655–661.

Clark, T. L., 1977: A small scale dynamic model using terrain-following coordinate transformation. *J. Comput. Phys.,* **24,** 186–215.

——, 1979: Numerical simulations with a three-dimensional cloud model. *J. Atmos. Sci.,* **36,** 2191–2215.

——, and R. Gall, 1982: Three-dimensional numerical model simulations of air flow over mountainous terrain: A comparison with observation. *Mon. Wea. Rev.,* **110,** 766–791.

——, and R. D. Farley, 1984: Severe downslope windstorm calculations in two and three spatial dimensions using anelastic interactive grid nesting. *J. Atmos. Sci.,* **41,** 329–350.

Cotton, W. R., G. D. Alexander, R. Hertenstein, R. L. Walko, R. L. McAnelly, and M. Nicholls, 1995: Cloud venting—A review and some new global annual estimates. *Earth–Sci. Rev.,* **39,** 169–206.

Fitzgerald, J. W., 1991: Marine aerosols: A review. *Atmos. Environ.,* **25A,** 533–545.

Flossmann, A. I., 1991: The scavenging of two different types of marine aerosol particles using a two-dimensional detailed cloud model. *Tellus,* **43B,** 301–321.

——, 1993: The effect of the impaction scavenging efficiency on the wet deposition by a convective warm cloud. *Tellus,* **45B,** 34–39.

——, 1994: A 2-D spectral model simulation of the scavenging of gaseous and particulate sulfate by a warm marine cloud. *J. Atmos. Res.,* **32,** 255–268.

——, and H. R. Pruppacher, 1988: A theoretical study of the wet removal of atmospheric pollutants. Part III. *J. Atmos. Sci.,* **45,** 1857–1871.

——, and W. Wobrock, 1996: Venting of gases by convective clouds. *J. Geophys. Res.,* **101,** 18 639–18 649.

——, W. D. Hall, and H. R. Pruppacher, 1985: A theoretical study of the wet removal of atmospheric pollutants. Part I. *J. Atmos. Sci.,* **42,** 582–606.

——, H. R. Pruppacher, and J. H. Topalian, 1987: A theoretical study of the wet removal of atmospheric pollutants. Part II. *J. Atmos. Sci.,* **44,** 2912–2923.

Hegg, D. A., L. F. Radke, and P. V. Hobbs, 1990: Particle production associated with marine clouds. *J. Geophys. Res.,* **95,** 13 917–13 926.

——, ——, and ——, 1991: Measurements of Aitken nuclei and cloud condensation nuclei in the marine atmosphere and their relation to the DMS-cloud-climate hypothesis. *J. Geophys. Res.,* **96,** 18 727–18 733.

Hall, W. D., 1980: A detailed microphysical model within a two-dimensional dynamic framework: Model description and preliminary results. *J. Atmos. Sci.,* **37,** 2486–2507.

Hobbs, P. V., 1993: *Aerosol-Cloud-Climate Interactions.* Academic Press, 233 pp.

Hoppel, W. A., 1992: The role of nonprecipitating cloud cycles and gas-to-particle conversion in the maintanance of the submicron aerosol size distribution over the tropical oceans. *Nucleation and Atmospheric Aerosols,* N. Fukuta and P. Wagner, Eds. A. Deepak, 9–18.

Jaenicke, R., 1988: Aerosol physics and chemistry. *Landolt-Boernstein: Zahlenwerte und Funktionen aus Naturwissenschaften und Technick,* Vol. 4b, G. Fischer, Ed., Springer, 391–457.

Junge, C. E., 1963: *Air Chemistry and Radioactivity.* Academic, 156 pp.

Kiang, C. S., D. Stauffer, V. A. Mohnen, J. Bricard, and D. Vigla, 1973: Heteromolecular nucleation theory applied to gas-to-particle conversion. *Atmos. Environ.,* **7,** 1279–1283.

Middleton, P., and C. S. Kiang, 1978: A kinetic aerosol model for the formation and growth of secondary sulfuric acid particles. *J. Aerosol Sci.,* **9,** 359–385.

Nicholls, S., and M. A. LeMone, 1980: The fair weather boundary layer in GATE: The relationship of subcloud fluxes and structure to the distribution and enhancement of cumulus clouds. *J. Atmos. Sci.,* **37,** 2051–2067.

Perry, K. D., and P. V. Hobbs, 1994: Further evidence for particle nucleation in clear air adjacent to marine cumulus clouds. *J. Geophys. Res.,* **99,** 22 803–22 818.

Radke, L. F., and P. V. Hobbs, 1991: Humidity and particle fields around some small cumulus clouds. *J. Atmos. Sci.,* **48,** 1190–1193.

Twomey, S., 1977: The influence of pollution on the shortwave albedo of clouds. *J. Atmos. Sci.,* **34,** 1149–1152.

Warner, C., J. Simpson, D. W. Martin, D. Suchman, F. R. Mosher, and R. F. Reinking, 1979: Shallow convection on Day 261 of GATE: Mesoscale arcs. *Mon. Wea. Rev.,* **107,** 1617–1635.